Topographical heterogeneity of K_{IR} currents in pericyte-containing microvessels of the rat retina: effect of diabetes

Kenji Matsushita[1] and Donald G. Puro[1,2]

[1]*Department of Ophthalmology & Visual Sciences and* [2]*Department of Molecular & Integrative Physiology, University of Michigan, Ann Arbor, MI 48105, USA*

Although inwardly rectifying potassium (K_{IR}) channels are known to have important functional roles in arteries and arterioles, knowledge of these channels in pericyte-containing microvessels is limited. A working hypothesis is that K_{IR} channel activity affects the membrane potential and thereby the contractile tone of abluminal pericytes whose contractions and relaxations may regulate capillary perfusion. Because pericyte function is thought to be particularly important in the retina, we used the perforated-patch technique to monitor the ionic currents of pericytes located on microvessels freshly isolated from the rat retina. In addition, because changes in ion channel function may contribute to microvascular dysfunction in the diabetic retina, we also recorded from pericyte-containing microvessels of streptozotocin-injected rats. Using barium to identify K_{IR} currents, we found that there is a topographical heterogeneity of these currents in the pericyte-containing microvasculature of the normal retina. Specifically, the K_{IR} current detected at distal locations is strongly rectifying, but the proximal K_{IR} current is weakly rectifying and has a smaller inward conductance. However, soon after the onset of diabetes, these differences diminish as the rectification and inward conductance of the proximal K_{IR} current increase. These diabetes-induced changes were reversed by an inhibitor of polyamine synthesis and could be mimicked by spermine, whose concentration is elevated in the diabetic eye. Hence, spermine is a candidate for mediating the effect of diabetes on the function of microvascular K_{IR} channels. In addition, our findings raise the possibility that functional changes in K_{IR} channels contribute to blood flow dysregulation in the diabetic retina.

(Received 7 February 2006; accepted after revision 30 March 2006; first published online 31 March 2006)
Corresponding author D. G. Puro: Department of Ophthalmology and Visual Sciences, University of Michigan, 1000 Wall Street, Ann Arbor, MI 48105, USA. Email: dgpuro@umich.edu

It has long been appreciated that pericyte-containing microvessels constitute the largest portion of the vasculature and are the sites of greatest resistance within the circulatory system. However, until recently these vessels were thought to play only a passive role in controlling perfusion. Even though it is well established that smooth muscle-encircled arteries have a major role in regulating blood flow, evidence is accumulating that capillary perfusion can also be actively regulated by abluminal pericytes whose contractions and relaxations cause adjacent lumens to constrict or dilate (Tilton, 1991; Hirschi & D'Amore, 1996; Schonfelder *et al.* 1998; Kawamura *et al.* 2003, 2004; Wu *et al.* 2003; Yamanishi *et al.* 2006).

While nearly all tissues have pericyte-containing microvessels, the function of this component of the circulatory system may be particularly important in the retina where a low capillary density minimizes interference with the passage of light, but leaves little functional reserve (Funk, 1997). Hence, a tight functional link between local perfusion and metabolic demand is especially critical in the retina. As an adaptive consequence, the retinal vasculature is highly specialized to enhance the local control of blood flow. For example, it lacks autonomic input (Ye *et al.* 1990), which in other vascular beds provides extrinsic CNS regulation. Also, the presence of endothelial tight junctions limits exposure of contractile mural cells to circulating vasoactive molecules. In addition, it is likely that the decentralized control of capillary perfusion is facilitated by the microvasculature of the retina having a higher density of pericytes than that of any other tissue (Shepro & Morel, 1993). Because of its specializations for enhancing the local control of capillary perfusion, the vasculature of the retina is especially useful for assessing hypotheses concerning

 DOI: 10.1113/jphysiol.2006.107102

the function of pericyte-containing microvessels. An experimental advantage of studying retinal microvessels is the ability to isolate viable microvascular complexes and to use techniques, such as patch-clamp recording, to analyse pericytes as components of a multicellular functional unit (Kawamura *et al.* 2003; Yamanishi *et al.* 2006; Wu *et al.* 2006; Yamanishi *et al.* 2006).

In this study using perforated-patch pipettes sealed onto the pericytes of freshly isolated retinal microvessels, we analysed inwardly rectifying potassium (K_{IR}) currents. Although knowledge of the function of K_{IR} channels in pericyte-containing microvessels is limited, there is substantial evidence from studies of smooth muscle-encircled vessels that these channels are important in the functioning of the circulatory system (Zaritsky *et al.* 2000; Chrissobolis & Sobey, 2003). For example, K_{IR} channels can regulate basal vascular tone by influencing the resting membrane potential and thereby the contractility of vascular myocytes (Edwards *et al.* 1988; Quayle *et al.* 1993). Also, because extracellular potassium levels rise when there is a mismatch between local perfusion and the demand for nutrients and oxygen, the unique ability of K_{IR} channels to increase their efflux of K^+ as the extracellular potassium concentration rises provides a mechanism for linking blood flow to metabolic need. In a variety of vascular beds, the mural cell hyperpolarization and relaxation induced by a potassium-induced K^+ efflux from K_{IR} channels is likely to underlie the phenomenon of metabolic vasodilatation (Edwards *et al.* 1988; Quayle *et al.* 1996; Zaritsky *et al.* 2000).

In addition to studying K_{IR} currents in retinal microvessels isolated from normal rats, we also monitored the ionic currents of pericytes located on microvessels from diabetic retinas. The effect of diabetes on the pericyte-containing retinal microvasculature is of keen interest because a key feature of diabetic retinopathy is the dysfunction and ultimately the death of microvascular cells (Mizutani *et al.* 1996; He & King, 2004). A working hypothesis of our study is that changes in the function of microvascular K_{IR} channels may contribute to the dysregulation of retinal blood flow observed early in the course of diabetes.

Here, we report that there is a topographical heterogeneity of K_{IR} channels in the pericyte-containing microvasculature of the normal retina. In the distal portion of these microvessels, the K_{IR} current shows strong inward rectification, i.e. there is relatively little outward current. In contrast, the K_{IR} current detected at proximal sites is weakly rectifying and has a smaller inward conductance. However, soon after the onset of streptozotocin-induced diabetes, these physiological differences diminish as the rectification and the inward conductance of proximal K_{IR} current increase. Suggestive of a role for polyamines, we observed similar effects on the physiology of K_{IR} currents in microvessels exposed to spermine, whose concentration is elevated in the vitreous of the diabetic eye (Nicoletti *et al.* 2003).

Methods

Animal use conformed to the guidelines of the Association for Research in Vision and Ophthalmology and was approved by the University of Michigan Committee on the Use and Care of Animals. Long-Evans rats (Charles River, Cambridge, MA, USA) were maintained on a 12 h alternating light–dark cycle and received food and water *ad libitum*.

Experimental model of diabetes

After an overnight fast, 4- to 5-week-old Long-Evans rats received an intraperitoneal injection of streptozotocin (STZ, 150 mg kg^{-1}) diluted in 0.8 ml citrate buffer. Immediately prior to the harvesting of the retinal microvessels, the blood glucose level was 427 ± 25 mg dl^{-1} ($n = 11$).

Microvessel isolation

Non-diabetic and diabetic rats (6–14 weeks old) were killed with a rising concentration of carbon dioxide. Retinas were rapidly removed, cut into quadrants and then incubated for 25–30 min at 30°C in 2.5 ml Earle's balanced salt solution supplemented with 0.5 mM EDTA, 20 mM glucose, 6 U papain (Worthington Biochemicals, Freehold, NJ, USA) and 2 mM cysteine; to maintain pH and oxygenation, 95% oxygen−5% carbon dioxide was bubbled into this solution. Subsequently, retinas were transferred to solution A, which consisted of 140 mM NaCl, 3 mM KCl, 1.8 mM $CaCl_2$, 0.8 mM $MgCl_2$, 10 mM Na-Hepes, 15 mM mannitol, and 5 mM glucose at pH 7.4 with osmolarity adjusted to 310 mosmol l^{-1}. Each piece of retina was then gently sandwiched between two glass coverslips (15 mm diameter, Warner Instrument Corp., Hamden, CT, USA). Retinal vessels adhered to the coverslip contacting the vitreal side of the retina.

Figure 1 shows a photomicrograph of a freshly isolated retinal microvascular complex. Cell viability is very high in microvessels isolated by this technique (Kodama *et al.* 2001; Sugiyama *et al.* 2004, 2005). Also, as demonstrated in time-lapse videos that supplement previous publications (Kawamura *et al.* 2003, 2004; Wu *et al.* 2003; Yamanishi *et al.* 2006), pericytes located on the isolated retinal microvessels show contractile responses to a variety of putative vasoactive signals.

Electrophysiology

The perforated-patch configuration of the patch-clamp technique was used to monitor currents in pericytes

Table 1. Composition of the perfusates (mM)

	Solutions			
Ingredients	A	B	C	D
KCl	3	3	10	97.5
NMDG-Cl	0	94.5	87.5	0
NaCl	140	43	43	43
$CaCl_2$	1.8	1.8	1.8	1.8
$MgCl_2$	0.8	0.8	0.8	0.8
Mannitol	15	15	15	15
Glucose	5	5	5	5
Na-Hepes	10	10	10	10

For each perfusate, the osmolarity was 310 mosmol l^{-1}, and the pH was 7.4.

located on freshly isolated microvessels. Experiments were performed at room temperature (22–24°C) on microvessels that had been isolated within 5 h. A coverslip containing microvessels was placed in a recording chamber (volume, 1 ml), which was perfused ($\sim$1.5 ml min^{-1}) with solutions from a gravity-fed system using multiple reservoirs. Solution A was the initial perfusate. Subsequently, we used other perfusates (Table 1), which were designed so that the concentration of potassium could be varied while the sodium and chloride concentrations, as well at the pH and osmolarity, were essentially unchanged. After adjustment of the pH to 7.4 with NaOH, the osmolarity of each perfusate was 310 mosmol l^{-1}, as measured by a vapour pressure osmometer (Wescor, Inc., Logan, UT, USA).

Vessels were examined at $\times$400 magnification with an inverted microscope equipped with phase-contrast optics. Arterioles had outer diameters of $> 12\,\mu$m and could be easily identified by the presence of 'doughnut-shaped' encircling smooth muscle cells (Fig. 1). Pericytes were identified by their characteristic 'bump on a log' appearance on the abluminal walls of microvessels (Kuwabara & Cogan, 1960; Sakagami *et al.* 1999; Oku *et al.* 2001). As *in situ* (Kuwabara & Cogan, 1960), the density of pericytes within the isolated retinal microvessels was less at distal, as compared with proximal, sites (Fig. 1). More specifically, we observed that at distances of $430 \pm 60\,\mu$m (sample size = 21) from an upstream smooth muscle-encircled arteriole, there were more than four pericyte somas per 100 μm segment. On the other hand, at more distal locations, the density of pericytes was less than 4 per 100 μm. The distal portion of the isolated microvasculature consisted of an extensively branched plexus that is difficult to quantify, but typically included several millimetres of microvessels.

In this study, a recording site was classified as being at a proximal location when there were at least six other pericyte somas located within 50 μm of the sampled pericyte, i.e. seven or more pericytes within a 100 μm segment in which the sampled pericyte was centrally positioned. A site was classified as distal if there were three or fewer other pericytes within 50 μm of the patch-clamped mural cell. Pericyte density, rather than the distance from an upstream arteriole, provided a useful parameter for classifying a recording site as being in the proximal or distal portion of the pericyte-containing microvasculature because isolated microvessels were not uncommonly detached from arterioles. More specifically, for the experiments reported here, 37% ($n = 27$) of the sampled proximal pericytes were located within an exclusively proximal microvascular segment; 68% ($n = 22$) of the sampled distal pericytes were located within exclusively distal segments. The proximal/distal criteria cited above also applied for the classification of sites within microvessels isolated from diabetic rats. We did not systematically record from intermediate locations in which the density of pericytes was 3–7 per 100 μm segment. After completion of each electrophysiological recording, the sampled microvessel was photographed; this permitted subsequent independent assessment of the density of

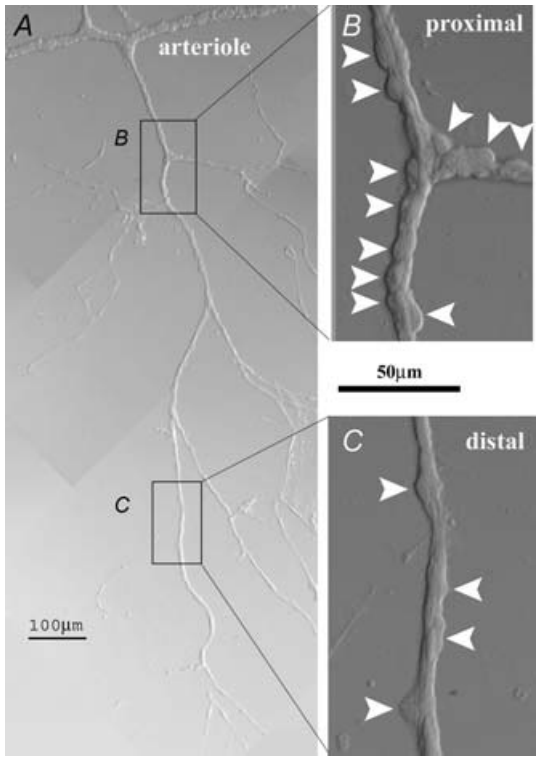

Figure 1. A vascular complex freshly isolated from the retina of an adult rat
A, low magnification photomicrograph of a smooth muscle-encircled vessel and pericyte-containing microvessels that branch from this arteriole. *B*, enlarged view of a portion of the proximal pericyte-containing microvasculature. Arrowheads show the pericyte somas. *C*, enlarged view of a portion of the distal pericyte-containing microvasculature. Arrowheads show the pericyte somas. As discussed in the text, the density of abluminal pericytes is less at distal microvascular sites.

pericytes, and thereby the microvascular location, i.e. proximal or distal, of the recording.

The recording pipette solution consisted of 50 mM KCl, 65 mM K_2SO_4, 6 mM $MgCl_2$, 10 mM K-Hepes, 60 μg ml^{-1} amphotericin B and 60 μg ml^{-1} nystatin at pH 7.4 with the osmolarity adjusted to 280 mosmol l^{-1}. The pipettes, which had resistances of $\sim$5 MΩ, were mounted in the holder of a patch-clamp amplifier (Axopatch 200B, Axon Instruments, Union City, CA, USA); seals of $\geq$ 10 GΩ were made to the cell bodies of pericytes. As amphotericin–nystatin perforated the patch of membrane, the access resistance to the pericytes studied decreased to less than 25 MΩ. Currents were filtered with a four-pole Bessel filter, digitally sampled using a DigiData 1200B acquisition system (Axon Instruments) and stored by a computer equipped with pCLAMP (version 8.2, Axon Instruments) and Origin (Version 7, OriginLab, Northampton, MA, USA) software for data analysis and graphics display.

Due to the presence of gap junction pathways in retinal microvessels (Oku *et al.* 2001; Wu *et al.* 2006), the currents detected by a perforated-patch pipette sealed onto a pericyte include not only those generated in the sampled pericyte, but also currents transmitted electrotonically from neighbouring vascular cells. Based on recordings made in the absence and presence of gap junction uncouplers, such as heptanol (Wu *et al.* 2006), octanol (Kawamura *et al.* 2002) and Gap-27 (S. Yamanishi and D. G. Puro, unpublished observations), it appears that approximately 95% of the current monitored via a perforated-patch pipette is generated by the microvascular neighbours of the sampled cell. Although space clamp would be more controlled in short microvessels, we recorded from pericytes located on microvessels of $>$ 300 μm in length because of the frequent occurrence of low membrane potentials and unstable recordings in shorter microvascular fragments. In fact, 50% of our recordings were from pericytes located on branching microvascular complexes that extended for $>$ 1 mm. However, as documented elsewhere (Sakagami *et al.* 1999; Li & Puro, 2001), the reversal potentials for conductances generated by potassium, chloride and non-specific cation channels in isolated retinal microvascular complexes closely match the calculated equilibrium potentials for these ions. Thus, it appears that the voltage within a microvessel can be clamped reasonably well at the sites containing the bulk of the ion channels contributing to the current detected in a sampled pericyte.

In order to determine current–voltage relations, currents were evoked by voltage steps controlled with pCLAMP software and measured as described previously (Sakagami *et al.* 1999). The zero-current potential was defined as the membrane potential. Adjustment for the calculated liquid junction potential (Barry, 1994) was made after data collection. Unless noted otherwise, the amplitude of the inward current at $-$50 mV from the potassium equilibrium potential (E_K) was used to calculate the inward K_{IR} conductance. Inward rectification was quantified by determining the rectification quotient, which was the absolute value of the ratio of the amplitude of the current at a voltage $-$50 mV from E_K to the amplitude of the outward current at +50 mV to E_K.

To calculate the current densities plotted in Figs 3*A* and 5, we used the method of Zhao & Santos-Sacchi (1998) to determine the membrane capacitance from the transient charge induced by a 10 mV hyperpolarization from a holding potential of $-$58 mV; pCLAMP software facilitated calculation of the area under the decaying capacitive current, i.e. the charge moved. The membrane capacitances used to calculate the current densities are in the legends of Figs 3*A* and 5. Under the various experimental conditions used in this study, there was no significant ($P > 0.3$) difference in the membrane capacitance determined from recordings of proximal *versus* distal pericytes. Also, there was no significant effect ($P > 0.3$) of barium, spermine, quercetin or diabetes on the membrane capacitance. On the other hand, the membrane capacitance measured during the perfusion of solution D (97.5 mM K^+) was significantly ($P < 0.001$) smaller; the cause for this effect is uncertain, but is likely to be due to voltage-dependent effects on the gap junction pathways that are extensive in the pericyte-containing microvasculature of the retina (Oku *et al.* 2001). In this investigation, we often studied K_{IR} currents in solution D (97.5 mM K^+) whose effect on the recorded membrane capacitance most likely reflects a decrease in the number of microvascular cells under voltage clamp; as a consequence, the monitored ionic currents in this solution facilitated our making of comparisons between the K_{IR} conductances generated at proximal *versus* distal locations within the retinal microvasculature.

Chemicals

Unless otherwise noted, chemicals were obtained from Sigma (St Louis, MO, USA).

Statistics and data analysis

Data are given as means $\pm$ S.E.M. Probability was evaluated by Student's *t* test. In Figs 2*B* and 4*B*, Origin software was used to generate the fits using the logistical equation, $y = A_2 + (A_1 - A_2)/[1 + (x/x_o)^p]$, where x_o is the centre; p is the power: A_1 is the initial Y value, and A_2 is the final Y value.

Results

The K_{IR} current of the distal microvasculature

To test the hypothesis that functional K_{IR} channels are expressed in the pericyte-containing microvasculature of the retina, we used the perforated-patch technique to monitor ionic currents in pericytes located on freshly isolated retinal microvessels. In order to identify inwardly rectifying potassium (K_{IR}) currents, we determined the current–voltage (I–V) relations in the absence and presence of various concentrations of barium, which blocks K_{IR} channels (Hille, 2001). In recordings from pericytes located in the distal portion of the retinal microvasculature (see Methods for criteria used to define distal and proximal sites), we observed that a strongly inwardly rectifying current was inhibited by barium in a dose-dependent manner with a half-maximally effective concentration of 10 μM (Fig. 2).

To further characterize the barium-sensitive current, we assessed the effect of various concentrations of extracellular potassium on the I–V relations of this conductance. Figure 3*A* summarizes our experiments using perfusates containing 3 mM (solution B), 10 mM (solution C) or 97.5 mM (solution D) potassium; these solutions were designed so that their sodium and chloride concentrations, as well as osmolarity and pH, were essentially the same (Table 1). As predicted for a potassium-selective current, the reversal potential of the inwardly rectifying barium-sensitive current closely matched the equilibrium potential for potassium (E_K). As is evident in Fig. 3*A*, the K_{IR} conductance increased as the extracellular potassium concentration was increased. One consequence of the K^+-dependent gating of K_{IR} channels is that an increase in $[K^+]_o$ induces an hyperpolarizing efflux of K^+. Consistent with this phenomenon, switching the perfusate from solution B (3 mM K^+) to solution C (10 mM K^+) caused the pericyte membrane potential to increase (Fig. 3*A*). In a series of experiments, this 7 mM increase in the concentration of potassium caused distal pericytes to hyperpolarize significantly ($P = 0.001$, $n = 12$), from -36 ± 2 mV to -50 ± 4 mV. Indicative of the importance of the barium-sensitive conductance, 2 mM barium prevented ($P < 0.001$; $n = 4$) this K^+-induced hyperpolarization.

The proximal K_{IR} current

In addition to recording from pericytes located at distal sites within the retinal microvasculature, we also monitored the ionic currents of proximal pericytes. As illustrated in Fig. 4*A*, we detected a barium-sensitive current at proximal sites. For this proximal current, the half-maximally effective inhibitory concentration of barium was 8 μM (Fig. 4*B*). Consistent with this barium-sensitive current being generated by potassium channels, its reversal potential was close to E_K over a range of potassium concentrations (Fig. 5). As with the

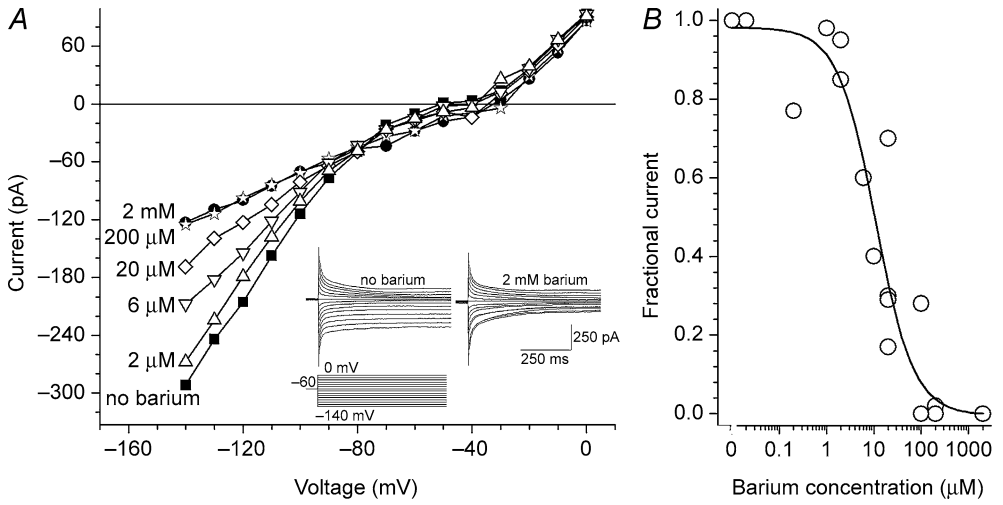

Figure 2. Effect of various concentrations of barium on the *I–V* relations determined from perforated-patch recordings from a pericyte located in the distal portion of the retinal microvasculature
To the left of each plot is shown the concentration of barium in the perfusate, which was solution C (10 mM K^+) supplemented with 0–2 mM $BaCl_2$. Inset, current traces generated in the absence or presence of 2 mM $BaCl_2$; also shown is the stimulus protocol. *B*, relationship between the barium concentration and the amplitude of the barium-sensitive current, which was measured in distally located pericytes held −45 mV from the equilibrium potential of potassium (E_K). The amplitude of current inhibited by 2 mM $BaCl_2$ was defined as the maximum barium-sensitive current. Each point represents one observation; data are from six distally located pericytes each of which was exposed to multiple concentrations of barium.

distal K_{IR} current, the conductance of the barium-sensitive current recorded from proximal pericytes increased with increasing potassium concentration in the perfusate (Fig. 5, inset).

We observed that raising the barium concentration from 100 μM to 2 mM caused only an additional $3.1 \pm 2.5\%$ ($n = 7$) inhibition of the inward current measured at -50 mV from E_K and a $0 \pm 3.1\%$ ($n = 7$) change in the outward current measured at $+50$ mV from E_K. Because some non-K_{IR} channels, such as ATP-sensitive K^+ channels and delayed rectifying K^+ channels (Hille, 2001) are sensitive to relatively high concentrations of barium, the minimal effects of $> 100\ \mu$M Ba^{2+} indicate that this divalent cation, even at 2 mM, blocked essentially only K_{IR} channels in the retinal microvasculature. Thus, in studies of isolated pericyte-containing retinal microvessels, it appears reasonable to use 2 mM Ba^{2+} to ensure that there is a complete block of K_{IR} channels over a wide range of voltages.

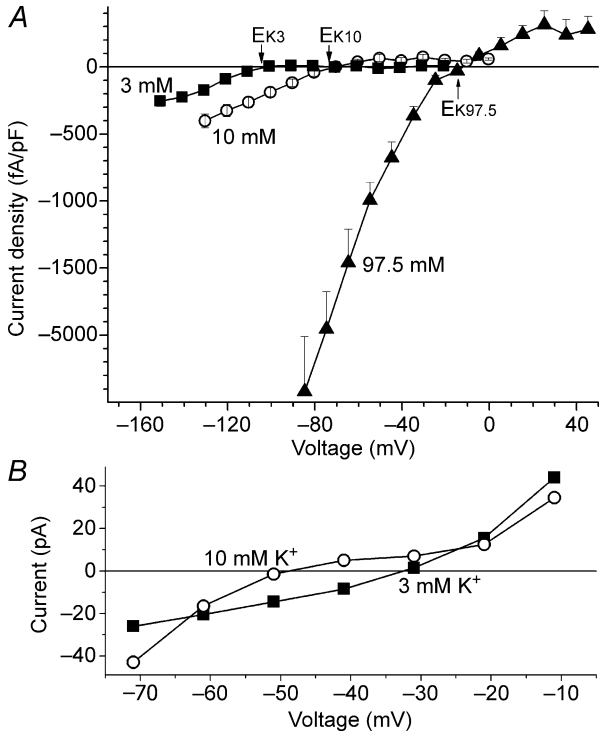

Figure 3. Effect of the extracellular potassium concentration on the currents recorded from pericytes located at distal sites in the retinal microvasculature

A, current densities of the barium-sensitive conductance in distal pericytes located on isolated microvessels perfused with solution B (3 mM K^+; $n = 4$), solution C (10 mM K^+; $n = 10$) or solution D (97.5 mM K^+; $n = 10$). The membrane capacitance, which was calculated as detailed in the Methods, was 274 ± 52 pF ($n = 4$), 249 ± 10 pF ($n = 10$) and 64 ± 22 pF ($n = 10$) in solutions B, C and D, respectively. For each of the potassium concentrations tested, the equilibrium potential for potassium (E_K) is shown. *B*, effect of increasing extracellular K^+ from 3 mM (solution B; ■) to 10 mM (solution C; ○) on the *I–V* relations of a distal pericyte.

Although we detected barium-sensitive currents at both proximal and distal sites within the pericyte-containing retinal microvasculature, we found that the current recorded from pericytes located at proximal differed from that detected at distal sites. As summarized in the inset of Fig. 5, the density of the proximal and distal K_{IR} currents differed significantly ($P < 0.05$) at each of the potassium concentrations tested. Over a wide range of potassium concentrations, the inward component of the proximal barium-sensitive current was smaller. On the other hand, the distal K_{IR} conductance showed significantly ($P < 0.001$) greater inward rectification; the rectification quotients (see Methods) were 3.8 ± 0.5 ($n = 10$) and 0.9 ± 0.2 ($n = 7$) for distal and proximal K_{IR} currents, respectively.

Consistent with proximal K_{IR} channels being more weakly rectifying and thereby having a greater basal efflux of K^+, the membrane potential of proximal pericytes was significantly ($P = 0.004$) more negative than the resting voltage of the distal pericytes; namely, the membrane potentials in solution A (3 mM K^+) were -45 ± 2 mV ($n = 27$) and -35 ± 2 mV ($n = 22$) for proximal and distal pericytes, respectively. Based on our perforated-patch recordings, we concluded that there is a topographical heterogeneity of the barium-sensitive currents in the pericyte-containing retinal microvasculature; at proximal sites, the K_{IR} current is relatively weakly rectifying and has a smaller inward conductance.

Shared features of the proximal and distal K_{IR} conductances

Despite the differences in the strength of rectification and the size of the inward conductance, we observed that the proximal and distal K_{IR} currents share some common physiological features. For example, they have similar sensitivities to barium, i.e. the IC_{50} was 10 μM and 8 μM for the distal and proximal currents, respectively (Figs 2*B* and 4*B*). Also, similar to the distal K_{IR} current, the conductance of the proximal K_{IR} current increased as the extracellular potassium concentration increased (Fig. 5). In addition, consistent with the hyperpolarizing effect of a K^+-induced increase in K^+ efflux from proximal K_{IR} channels, switching the perfusate from solution B (3 mM K^+) to solution C (10 mM K^+) caused the membrane potential of proximally located pericytes to increase significantly ($P < 0.001$, $n = 12$), from -45 ± 2 mV to -59 ± 2 mV. Indicative of the role of the barium-sensitive conductance, this potassium-induced hyperpolarization of proximal pericytes was blocked ($P < 0.001$; $n = 4$) by 2 mM barium. As noted, a 7 mM rise in the potassium concentration also caused a 14 mV hyperpolarization of distal pericytes. Thus, the K_{IR} currents of the proximal and distal portions of the pericyte-containing retinal

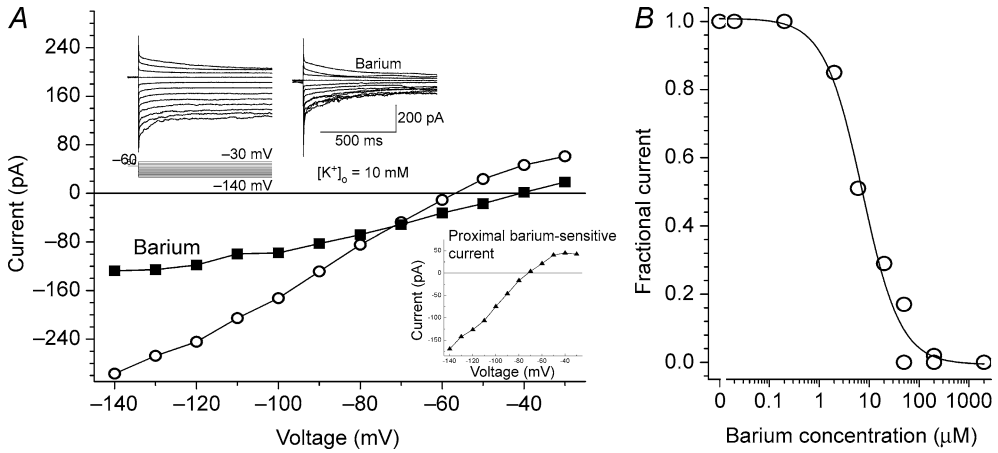

Figure 4. Effects of extracellular barium on currents recorded from pericytes located at proximal sites in the pericyte-containing retinal microvasculature
A, *I–V* relations of currents during perfusion of solution C (10 mM K^+) in the absence (○) and presence (■) of 2 mM $BaCl_2$. Upper inset, current traces from which the *I–V* plots were generated. Also shown is the stimulus protocol. Lower inset, plot of the difference between the *I–V* curves. *B*, relationship between the barium concentration and the amplitude of the proximal barium-sensitive current, which was measured in proximally located pericytes held −45 mV from E_K. Data are from five proximally located pericytes each of which was exposed to multiple concentrations of barium.

microvasculature share a number of physiological similarities.

Proximal K_{IR} currents and distal membrane potentials

In a recent study of the electrotonic architecture of pericyte-containing retinal microvessels, we demonstrated that locally generated voltage changes spread via gap junction pathways to distant sites in a microvascular complex (Wu *et al.* 2006). Based on the findings of the present study, we hypothesized that the hyperpolarization generated by K^+ effluxing via weakly rectifying proximal K_{IR} channels should have a widespread influence on the membrane potentials of microvascular cells. To begin to assess this hypothesis, we compared the resting membrane potentials of pericytes that were either located on large microvascular complexes that included both proximal and distal regions or were on small microvascular segments that included only proximal or distal regions. We found that in isolated proximal segments, the pericyte voltage was -44 ± 3 mV ($n = 10$; in solution A). In contrast, the membrane potential of the pericytes on isolated distal segments was -32 ± 3 mV ($n = 13$); this was a significant ($P = 0.011$) difference. However, in large microvascular complexes the pericyte membrane potentials were -46 ± 3 mV ($n = 10$) and

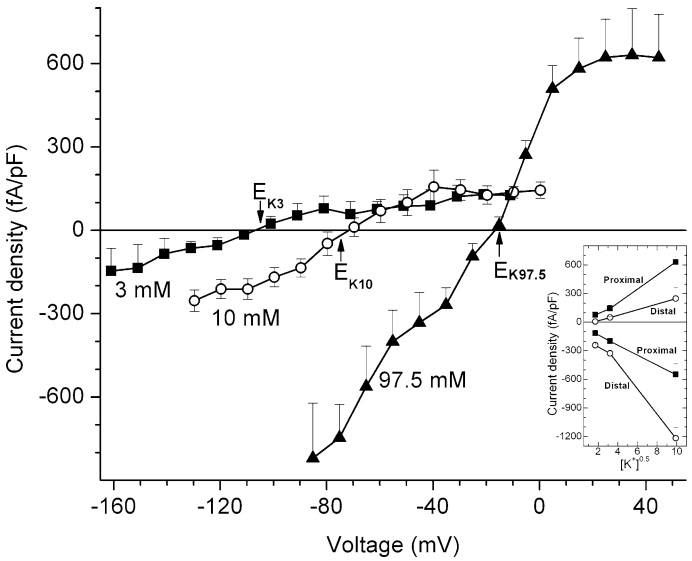

Figure 5. Effect of extracellular potassium concentration on barium-sensitive conductance recorded from pericytes located at proximal sites within the retinal microvasculature
Plot shows the relationship between current density and voltage for the barium-sensitive conductances recorded in solution B (3 mM K^+; $n = 4$), solution C (10 mM K^+; $n = 11$) or solution D (97.5 mM K^+; $n = 7$). For each of the tested potassium concentrations, the equilibrium potential for potassium (E_K) is shown. From perforated-patch recordings of distal pericytes, the calculated membrane capacitance was 220 ± 46 pF ($n = 4$), 325 ± 70 pF ($n = 13$) and 59 ± 25 pF ($n = 7$) in solutions B, C and D, respectively. Inset, the relationship between the square root of the extracellular potassium concentration and the current density. Current densities, which were determined at ±45 mV from E_K, are shown for inward and outward barium-sensitive conductances recorded at distal (○) and proximal (■) sites. The *P* values for proximal and distal inward current densities being different were 0.032, 0.016 and 0.001 at 3 mM, 10 mM and 97.5 mM, respectively. The *P* values for proximal and distal outward current densities being different were 0.050, 0.026 and 0.010 at 3 mM, 10 mM and 97.5 mM, respectively.

-41 ± 2 mV ($n = 8$: $P = 0.2$) at proximal and distal sites, respectively. These observations indicate that the hyperpolarization generated by K^+ effluxing through weakly rectifying proximal K_{IR} channels spreads electrotonically to distal sites in the pericyte-containing retinal microvasculature. Thus, we predict that *in vivo* membrane potentials throughout much of a microvascular complex are not significantly different when gap junctions are opened. However, when extracellular ATP, angiotensin II or endothelin-1 inhibit cell-to-cell communication within retinal microvessels (Kawamura *et al.* 2002, 2003, 2004), the electrotonic transmission of voltage would be minimized, and as a consequence, we postulate that the proximal/distal disparity in K_{IR}-generated hyperpolarization would be manifested.

K_{IR} currents in diabetic microvessels

In addition to recording K_{IR} currents in microvessels of the normal retina, we also obtained perforated-patch recordings from pericytes located on retinal microvessels of diabetic rats. Our working hypothesis was that diabetes, which is known to cause dysregulation of retinal blood flow, alters the activity of microvascular K_{IR} channels. To begin to test this possibility, we analysed the barium-sensitive currents in microvessels freshly isolated from the retinas of rats that had been made diabetic by streptozotocin for up to 4 months. Of importance, our pericyte density criteria used to classify microvascular sites as proximal or distal was unaffected by ≤ 4 months of experimental diabetes; this was consistent with *in vivo* studies showing that the loss of retinal pericytes is minimal during this early period after the onset of experimental diabetes (Tilton *et al.* 1986; Mizutani *et al.* 1996).

In electrophysiological experiments (Fig. 6), we found that 60 ± 8 days ($n = 5$) of diabetes resulted in a significant ($P < 0.001$) increase in K_{IR} rectification; the rectification quotients of the proximal K_{IR} current in diabetic and non-diabetic microvessels were 11.3 ± 0.9 ($n = 5$) and 0.9 ± 0.2 ($n = 7$). In addition, there was a significant ($P < 0.001$) increase in the inward conductance of the K_{IR} current recorded in pericytes located in the proximal portion of diabetic retinal microvessels. In contrast to the diabetes-induced change in the proximal K_{IR} currents, we did not detect an effect of diabetes on the K_{IR} current recorded from distal pericytes (Fig. 6, inset). In addition, suggestive that diabetes predominantly affects K_{IR} channels and not other channel types, recordings from proximal pericytes showed that diabetes did not significantly ($P = 0.6$; $n = 5$) alter the conductance that was insensitive to barium. Thus, based on our perforated-patch recordings, we concluded that diabetes affects K_{IR} channels in the proximal portion of the pericyte-containing retinal microvasculature.

Associated with the diabetes-induced strengthening of rectification and the consequent decrease in basal K^+ efflux from proximal K_{IR} channels, the membrane potential of proximal pericytes was 7 ± 1 mV less negative ($P = 0.004$) in diabetic, as compared with the non-diabetic, microvessels. Specifically, pericytes located on the proximal portion of microvessels isolated 60 ± 8 days after the onset of diabetes had a membrane potential of -38 ± 1 mV ($n = 5$; in solution A) while the voltage of proximal pericytes in normal microvessels was -45 ± 2 mV ($n = 27$). This diabetes-induced depolarization detected in proximal pericytes exposed to a 3 mM K^+ perfusate (solution A) is consistent with diabetes affecting the outward K_{IR} current under relatively physiological conditions. As a result of the diabetes-induced

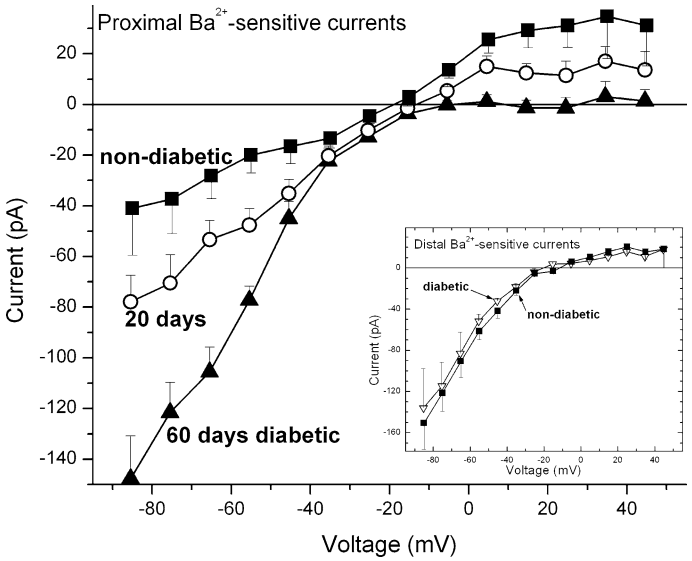

Figure 6. Effect of diabetes on the microvascular K_{IR} current
I–V relations for the barium-sensitive current recorded at proximal sites of microvessels isolated from normal rats (■; $n = 7$) and from streptozotocin-injected rats that were diabetic for 20 ± 3 days (○, $n = 9$) or 60 ± 8 days (▲, $n = 5$). Recordings were in solution D (97.5 mM K^+). Inset, *I–V* plots for the barium-sensitive currents recorded in solution D at distal sites in microvessels from non-diabetic rats (■, $n = 10$) and rats that had been diabetic for 69 ± 7 days (▽, $n = 2$); this duration of diabetes was not significantly ($P = 0.5$) different from that of the '60 day' group.

depolarization of proximal pericytes, diabetic microvessels did not have a significant ($P = 0.6$) difference in the resting membrane potentials of their proximal (-38 ± 1 mV; $n = 5$; in solution A) and distal (-36 ± 3 mV; $n = 3$) pericytes. Taken together, our perforated-patch recordings indicate that the topographical heterogeneity of K_{IR} currents becomes minimal in diabetic retinal microvessels.

Role of spermine in diabetic microvessels

By what mechanism does diabetes affect proximal K_{IR} channels? We considered the possibility that spermine plays a role. This polyamine was of interest because its concentration is increased in the diabetic eye (Nicoletti *et al.* 2003) and it is known to regulate K_{IR} channel function (Lopatin *et al.* 1994; Xie *et al.* 2005). To begin to assess the possible role of spermine, microvessels isolated from the retinas of non-diabetic rats were exposed to this polyamine. Our recordings from proximally located pericytes showed that exposure to spermine (5 mM) significantly ($P = 0.003$) increased the rectification of the K_{IR} current; specifically the rectification quotient increased from 0.9 ± 0.2 ($n = 7$) to 6.4 ± 0.7 ($n = 4$). In addition, exposure to spermine was associated with a significant ($P = 0.022$) increase in the inward conductance of the barium-sensitive current (Fig. 7*A*). These changes were induced within 15 min of the onset of spermine exposure and reversed within 20 min of the washout of this polyamine. We also found that the resting membrane potential of proximal pericytes exposed to 5 mM spermine was -36 ± 3 mV ($n = 6$) in solution A (3 mM K^+). This was significantly ($P = 0.004$) less that the -45 ± 2 mV ($n = 27$) voltage of pericytes in microvessels perfused with solution A without spermine. The spermine-induced depolarization of proximal pericytes is consistent with this polyamine inhibiting the outward K_{IR} current at physiological concentrations of extracellular K^+. From our experiments using spermine, we concluded that the effects of this polyamine on the proximal K_{IR} current were qualitatively similar to those of diabetes.

To further test the hypothesis that the diabetes-induced effects on proximal K_{IR} channels involve polyamines, microvessels freshly isolated from diabetic retinas were exposed to DL-α-difluoromethylornithine (DFMO, 5 mM in solution A), which reduces polyamine synthesis by inhibiting ornithine decarboxylase (ODC). In this series of experiments, we exposed diabetic microvessels to solution A without or with DFMO for 4–5 h at 37°C or overnight at room temperature. As shown in Fig. 7*B*, the proximal K_{IR} current in the DFMO-treated diabetic

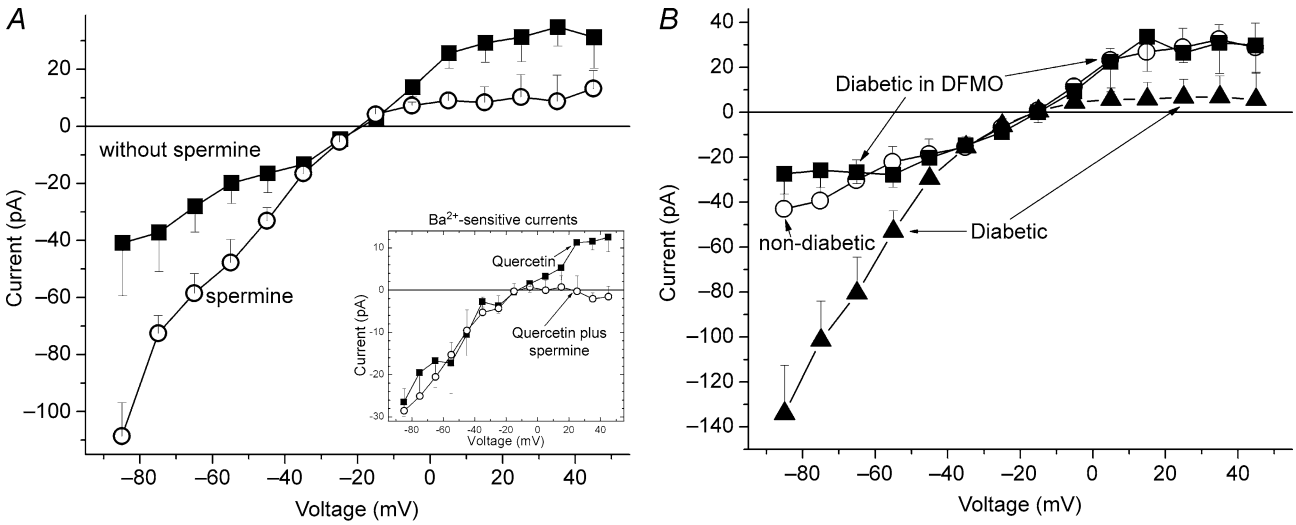

Figure 7. Effects of spermine and DFMO on the proximal K_{IR} current
A, *I–V* relations for the proximal barium-sensitive current in the absence (■; $n = 7$) and presence (○; $n = 6$) of 5 mM spermine in solution D (97.5 mM K^+); in the spermine group, microvessels were exposed to this polyamine for ≥ 15 min. Inset, *I–V* plots of the proximal barium-sensitive current in solution D supplemented with quercetin (100 μM) minus (■; $n = 2$) or plus 5 mM spermine (○; $n = 4$). *I–V* relations were generated after 15–20 min of exposure to quercetin; when used, spermine was in the perfusate for ≥ 15 min. In proximal pericytes, the barium-sensitive currents recorded in the absence or presence of quercetin did not have significantly ($P = 0.6$) different inward conductances or rectification quotients. *B*, *I–V* relations of the barium-sensitive current recorded at proximal sites in retinal microvessels that were either (1) isolated from diabetic rats (▲; $n = 9$; 86 ± 11 days of diabetes) and assayed in solution D (97.5 mM K^+), or (2) isolated from diabetic rats and as detailed in the text, exposed to solution D (97.5 mM K^+) supplemented with 5 mM DFMO (■; $n = 4$; 88 ± 9 days of diabetes), or (3) isolated from non-diabetic rats (○; $n = 7$; assayed in solution D). The duration of diabetes for groups (1) and (2) was not significantly ($P = 0.9$) different.

microvessels showed weaker rectification ($P = 0.001$) and a smaller inward conductance ($P = 0.009$). Specifically, we found that in solution D, DFMO significantly ($P = 0.0071$) decreased the rectification quotient from 11.7 ± 2.3 ($n = 8$; 86 ± 12 days of diabetes) to 0.9 ± 0.4 ($n = 4$; 88 ± 9 days of diabetes); DFMO also decreased the inward conductance by $66 \pm 6\%$ ($P = 0.007$). Importantly, we also observed that as compared with diabetic microvessels assayed within 5 h of isolation from the retina, microvessels maintained in solution A for up to 20 h ($n = 4$) did not have a significantly different inward conductance ($P = 0.2$) or rectification quotient ($P = 0.8$) when subsequently assayed in solution D. Thus, DFMO reversed the effects of diabetes on the proximal K_{IR} current. Consistent with DFMO causing an increase in the outward K_{IR} current at physiological concentrations of extracellular K^+, the resting membrane potential in solution A (3 mM K^+) of pericytes located on the proximal portion of the DFMO-treated diabetic microvessels was -47 ± 2 mV ($n = 5$), which was significantly ($P = 0.002$) more negative that the -39 ± 1 mV ($n = 8$) voltage of proximal pericytes located on diabetic microvessels (86 ± 12 days post-streptozotocin injection) that had not been exposed to this ODC inhibitor. Also of interest, the membrane potential of proximal pericytes in DFMO-treated diabetic microvessels (-47 ± 2 mV; $n = 5$) was not significantly ($P = 0.5$) different from the voltage of pericytes in the non-diabetic microvessels (-45 ± 2 mV; $n = 27$). In conclusion, the experiments in which normal microvessels were exposed to spermine and diabetic microvessels were treated with DFMO provided evidence to support the hypothesis that spermine mediates the effects of diabetes on the K_{IR} channels of the proximal pericyte-containing retinal microvasculature.

How does exposure to extracellular spermine alter microvascular K_{IR} channel function? Not only is it well established that the direct interaction of spermine with the intracellular portion of K_{IR} channels blocks K^+ efflux (Lopatin *et al.* 1994), but it is also likely that intracellular spermine interacts with phosphatidylinositol 4,5-bisphosphate (PIP_2) whose binding to these channels enhances K_{IR} channel activity (Xie *et al.* 2005). Because these actions occur intracellularly, it seems likely that the spermine in our perfusate must enter microvascular cells in order to regulate the K_{IR} channel function. However, in this study we were unable to assess spermine uptake due to the lack of specific inhibitors of hemi-junctions and polyamine transporters, which provide pathways for spermine influx (Gilad & Gilad, 1991; Cullis *et al.* 1999; Enkvetchakul *et al.* 2003). On the other hand, we were able to begin to test the possibility that PIP_2 plays a role in mediating the spermine-induced increase in the inward conductance of the proximal K_{IR} current. As illustrated in the inset of Fig. 7*A*, we found that spermine did not augment the proximal inward conductance when non-diabetic microvessels were exposed for 4–15 min to quercetin (100 μM), which is an inhibitor of PIP_2 synthesis (Walker *et al.* 2000). In addition to quercetin blocking this effect of spermine in the 97.5 mM K^+ solution (solution D), we also observed that in a 3 mM K^+ perfusate (solution A), the spermine-induced augmentation of the inward K_{IR} conductance detected in proximal pericytes was eliminated ($P < 0.001$) when microvessels were exposed to quercetin ($n = 6$). In contrast to quercetin's inhibition of the ability of spermine to increase the inward K_{IR} current, the PIP_2 inhibitor did not prevent this polyamine from increasing the rectification of the proximal K_{IR} current (Fig. 7*A*, inset). This observation is consistent with PIP_2 not being involved with spermine's direct block of K^+ effluxing through K_{IR} channels. Thus, our experiments indicate that spermine affects microvascular K_{IR} channels by two mechanisms, only one of which is blocked by quercetin.

Discussion

The results of our perforated-patch recordings from pericytes located on freshly isolated retinal microvessels show that there is a topographical heterogeneity of the K_{IR} currents. At distal sites within this microvasculature, the K_{IR} current showed strong inward rectification. In contrast, the proximal K_{IR} current was weakly rectifying and had a smaller inward conductance. However, soon after the onset of streptozotocin-induced diabetes, these functional differences became minimal as the rectification and the inward conductance of the proximal K_{IR} current increased markedly. Of possible mechanistic significance, these diabetes-induced effects were qualitatively mimicked by spermine whose concentration is elevated in the diabetic eye (Nicoletti *et al.* 2003). Also suggestive of a role for spermine, exposure of diabetic microvessels to a pharmacological inhibitor of polyamine synthesis significantly diminished the rectification and the inward conductance of the proximal K_{IR} current. Taken together, our experiments indicate that: (1) there are substantial functional differences in the K_{IR} channels expressed at proximal, as compared with distal, sites within the pericyte-containing microvasculature of the normal retina; (2) this heterogeneity is minimized early in the course of diabetes; and (3) spermine mimics the effects of diabetes on the physiology of proximal K_{IR} channels.

Although there are few studies of K_{IR} currents in pericyte-containing microvessels, there is substantial evidence from studies of larger vessels that K_{IR} channels are important in the circulatory system. For example, in arterioles from a variety of tissues, the K^+-dependent gating of K_{IR} channels plays a significant role in mediating a vasodilatory response to a rise in the extracellular potassium concentration. Abluminal

myocytes relax as K^+ effluxing from K_{IR} channels causes their membrane potentials to rise, their voltage-dependent calcium channels to close and subsequently their intracellular concentration of calcium to fall (Chrissobolis & Sobey, 2003). Similarly, we observed in retinal microvessels that raising extracellular K^+ from 3 to 10 mM increased the outward K_{IR} current and induced a barium-sensitive hyperpolarization of pericytes. Thus, vessels ensheathed by pericytes, as well as those encircled by smooth muscle cells, are responsive to metabolic conditions that cause $[K^+]_o$ to rise.

This study also suggests that there are similarities in the functional organization of the pericyte-containing and the smooth muscle-encircled vasculatures. For example, similar to our observation that the inward K_{IR} conductance is greater at distal sites within pericyte-containing microvessels, studies of coronary and renal arteries indicate that the inward K_{IR} conductance is larger in the smaller diameter, distal portions of these vessels (Quayle *et al.* 1996; Chilton & Loutzenhiser, 2001). In addition to this topographical heterogeneity, the K_{IR} currents of at least some arterioles also are heterogeneous with respect to their strength of rectification. Specifically, the K_{IR} current recorded in cerebral arterioles is strongly rectifying at proximal sites, but weakly rectifying at distal locations (Edwards *et al.* 1988). In our study, we also found a topographical heterogeneity, although in the retinal microvasculature the proximal K_{IR} current is weakly rectifying and the distal current is strongly rectifying.

Topological differences in the rectification of K_{IR} channels almost certainly have functional consequences. For example, the basal hyperpolarizing effect of K^+ effluxing through weakly rectifying K_{IR} channels should diminish the voltage change and the contractile response induced by vasoactive signals. Conversely, the minimal efflux of K^+ via strongly rectifying K_{IR} channels would provide little hyperpolarization to counterbalance an induced depolarization. Based on these considerations, we postulate that the distal portion of the pericyte-containing retinal microvasculature is more responsive to depolarizing inputs than its proximal counterpart. In this way, the topographical heterogeneity of microvascular K_{IR} channels in retinal microvessels may facilitate the decentralized control of capillary perfusion in the retina.

What are the consequences of diabetes causing the proximal K_{IR} current in the retinal microvasculature to become similar to the distal K_{IR} current? One predicted effect of a diabetes-induced enhancement of rectification and the consequent reduction in K^+ efflux via proximally located K_{IR} channels is a lowering of the resting membrane potential of proximal pericytes. In agreement with this prediction, the voltage of proximal pericytes in retinal microvessels of rats that had been diabetic for approximately 2 months was 7 ± 1 mV less negative ($P = 0.004$) than the membrane potential of proximal pericytes on non-diabetic microvessels. Although it remains to be demonstrated, this depolarization and the resulting increase in contractile tone may play a role in the decrease in microvascular perfusion observed early in the course of diabetes (Grunwald, 1996). In addition, vasoconstriction in the diabetic retina may be increased as the diabetes-induced decrease in K^+ efflux via proximal K_{IR} channels enhances the effectiveness of depolarizing stimuli, such as endothelin-1, which is up-regulated in the diabetic retina (Takagi *et al.* 1996; Chakravarthy *et al.* 1997). Also, because the activity of K_{IR} channels is reported to be linked with the proliferation of vascular cells (Karkanis *et al.* 2003), a speculative possibility is that the diabetes-induced change in K_{IR} channel function plays a role in retinal neovascularization, which is a major diabetic complication.

By what mechanism does diabetes alter the proximal K_{IR} current in pericyte-containing retinal microvessels? Our experiments suggest that a role may be played by spermine whose concentration is elevated in the vitreous of diabetics (Nicoletti *et al.* 2003). For example, we found that this polyamine qualitatively mimicked the effects of diabetes, i.e. it induced greater rectification and increased the inward conductance of the proximal K_{IR} current. In addition, exposure of diabetic microvessels to an inhibitor of polyamine synthesis reversed the diabetes-induced changes in the proximal K_{IR} current. Although future studies are needed to elucidate the mechanisms by which spermine regulates K_{IR} channels in the retinal microvasculature, the observed spermine-induced decrease in outward K_{IR} current is consistent with classic studies showing that this polyamine directly interacts with the cytoplasmic side of K_{IR} channels to block the efflux of K^+ (Lopatin *et al.* 1994). On the other hand, less is known about how spermine would increase the inward K_{IR} conductance in retinal microvessels. However, evidence is accumulating that a spermine-induced activation of K_{IR} channels is mediated by PIP_2 whose binding to these channels increases K^+ flux (Zhang *et al.* 1999). In a number of cell types, a link between this polyamine and PIP_2 is that the synthesis of this phospholipid can be increased by spermine (Coburn *et al.* 2002). Another association between spermine and PIP_2 is the recent demonstration that the binding of PIP_2 to a K_{IR} channel is enhanced by this polyamine (Xie *et al.* 2005). Taken together, spermine's dual effects on K_{IR} channels, i.e. blocking K^+ efflux and increasing channel activation, suggest the parsimonious scenario in which this polyamine induces functional changes in the K_{IR} channels of the proximal microvasculature. Perhaps, topological differences in spermine levels account for the proximal/distal heterogeneity of K_{IR} channel function in the retinal microvasculature. On the other hand, our experimental findings do not exclude an alternative possibility in which exposure to spermine

results in a switch in the type of K_{IR} channel expressed in the proximal portion of the retina's pericyte-containing microvasculature.

Our analysis of K_{IR} currents is based on experiments using freshly isolated microvessels. One advantage of studying isolated microvessels is that the patch-clamp technique can be used to monitor the ionic currents of pericytes. At present, this electrophysiological technique has not been successfully applied to the analysis of pericyte-containing microvessels *in situ*. An additional experimental advantage of isolated microvessels is the ability to study the effects of spermine, potassium and barium without confounding effects mediated by non-vascular cells. In future studies, freshly isolated microvessels may permit analyses to determine which types of K_{IR} channels are expressed at various sites in normal, diabetic and spermine-treated microvessels. However, despite advantages, caution must be exercised when making conclusions based on the study of isolated vessels. For example, the microvessels used in this study were not internally perfused and, thus, the possible effects of blood flow on the function of K_{IR} channels were not assessed. In addition, until studies are done on retinal microvessels *in situ*, we cannot exclude the possibility that our procedure for isolating microvessels alters the function of K_{IR} channels. However, despite caveats, our experimental preparation has facilitated the detection of a topographical heterogeneity of K_{IR} currents and has also led to the recognition that diabetes alters the physiological characteristics of these currents.

In summary, we report that the K_{IR} current detected in the proximal portion of the pericyte-containing retinal microvasculature is weakly rectifying. In contrast, the distal K_{IR} current is strongly rectifying and has a greater inward conductance. However, early in the course of diabetes, these functional differences wane as the physiology of the proximal K_{IR} current becomes similar to that of the distal K_{IR} current. We also found that these diabetes-induced changes in the proximal K_{IR} current were mimicked by spermine whose concentration is likely to be elevated in the diabetic retina. In addition, our experimental observations raise the possibility that vascular dysfunction in the diabetic retina may, in part, be caused by functional changes in K_{IR} channels of the pericyte-containing microvasculature.

References

Barry PH (1994). JPCalc, a software package for calculating liquid junction potential corrections in patch-clamp, intracellular, epithelial and bilayer measurements and for correcting junction potential measurements. *J Neurosci Meth* **51**, 107–116.

Chakravarthy U, Hayes RG, Stitt AW & Douglas A (1997). Endothelin expression in ocular tissues of diabetic and insulin-treated rats. *Invest Ophthalmol Vis Sci* **38**, 2144–2151.

Chilton L & Loutzenhiser R (2001). Functional evidence for an inward rectifier potassium current in rat renal afferent arterioles. *Circ Res* **88**, 152–158.

Chrissobolis S & Sobey CG (2003). Inwardly rectifying potassium channels in the regulation of vascular tone. *Curr Drug Targets* **4**, 281–289.

Coburn RF, Jones DH, Morgan CP, Baron CB & Cockcroft S (2002). Spermine increases phosphatidylinositol 4,5-bisphosphate content in permeabilized and nonpermeabilized HL60 cells. *Biochim Biophys Acta* **1584**, 20–30.

Cullis PM, Green RE, Merson-Davies L & Travis N (1999). Probing the mechanism of transport and compartmentalisation of polyamines in mammalian cells. *Chem Biol* **6**, 717–729.

Edwards FR, Hirst GD & Silverberg GD (1988). Inward rectification in rat cerebral arterioles; involvement of potassium ions in autoregulation. *J Physiol* **404**, 455–466.

Enkvetchakul D, Ebihara L & Nichols CG (2003). Polyamine flux in Xenopus oocytes through hemi-gap junctional channels. *J Physiol* **553**, 95–100.

Funk RH (1997). Blood supply of the retina. *Ophthalmic Res* **29**, 320–325.

Gilad GM & Gilad VH (1991). Polyamine uptake, binding and release in rat brain. *Eur J Pharmacol* **193**, 41–46.

Grunwald JE & Bursell S (1996). Hemodynamic changes as early markers of diabetic retinopathy. *Curr Opin Endocrinol Diabetes* **3**, 298–306.

He Z & King GL (2004). Microvascular complications of diabetes. *Endocrinol Metab Clin North Am* **33**, 215–238. xi–xii.

Hille B (2001). *Ion Channels of Excitable Membranes*. Sinauer Associates, Inc, Sunderland, Massachusetts.

Hirschi KK & D'Amore PA (1996). Pericytes in the microvasculature. *Cardiovasc Res* **32**, 687–698.

Karkanis T, Li S, Pickering JG & Sims SM (2003). Plasticity of KIR channels in human smooth muscle cells from internal thoracic artery. *Am J Physiol Heart Circ Physiol* **284**, H2325–H2334.

Kawamura H, Kobayashi M, Li Q, Yamanishi S, Katsumura K, Minami M, Wu DM & Puro DG (2004). Effects of angiotensin II on the pericyte-containing microvasculature of the rat retina. *J Physiol* **561**, 671–683.

Kawamura H, Oku H, Li Q, Sakagami K & Puro DG (2002). Endothelin-induced changes in the physiology of retinal pericytes. *Invest Ophthalmol Vis Sci* **43**, 882–888.

Kawamura H, Sugiyama T, Wu DM, Kobayashi M, Yamanishi S, Katsumura K & Puro DG (2003). ATP: a vasoactive signal in the pericyte-containing microvasculature of the rat retina. *J Physiol* **551**, 787–799.

Kodama T, Oku H, Kawamura H, Sakagami K & Puro DG (2001). Platelet-derived growth factor-BB: a survival factor for the retinal microvasculature during periods of metabolic compromise. *Curr Eye Res* **23**, 93–97.

Kuwabara T & Cogan D (1960). Studies of retinal vascular patterns. 1: normal architecture. *Arch Ophthalmol* **64**, 904–911.

Li Q & Puro DG (2001). Adenosine activates ATP-sensitive K^+ currents in pericytes of rat retinal microvessels: role of A1 and A2a receptors. *Brain Res* **907**, 93–99.

Lopatin AN, Makhina EN & Nichols CG (1994). Potassium channel block by cytoplasmic polyamines as the mechanism of intrinsic rectification. *Nature* **372**, 366–369.

Mizutani M, Kern TS & Lorenzi M (1996). Accelerated death of retinal microvascular cells in human and experimental diabetic retinopathy. *J Clin Invest* **97**, 2883–2890.

Nicoletti R, Venza I, Ceci G, Visalli M, Teti D & Reibaldi A (2003). Vitreous polyamines spermidine, putrescine, and spermine in human proliferative disorders of the retina. *Br J Ophthalmol* **87**, 1038–1042.

Oku H, Kodama T, Sakagami K & Puro DG (2001). Diabetes-induced disruption of gap junction pathways within the retinal microvasculature. *Invest Ophthalmol Vis Sci* **42**, 1915–1920.

Quayle JM, Dart C & Standen NB (1996). The properties and distribution of inward rectifier potassium currents in pig coronary arterial smooth muscle. *J Physiol* **494**, 715–726.

Quayle JM, McCarron JG, Brayden JE & Nelson MT (1993). Inward rectifier K^+ currents in smooth muscle cells from rat resistance-sized cerebral arteries. *Am J Physiol* **265**, C1363–C1370.

Sakagami K, Wu DM & Puro DG (1999). Physiology of rat retinal pericytes: modulation of ion channel activity by serum-derived molecules. *J Physiol* **521**, 637–650.

Schonfelder U, Hofer A, Paul M & Funk RH (1998). In situ observation of living pericytes in rat retinal capillaries. *Microvasc Res* **56**, 22–29.

Shepro D & Morel NM (1993). Pericyte physiology. *FASEB J* **7**, 1031–1038.

Sugiyama T, Kawamura H, Yamanishi S, Kobayashi M, Katsumura K & Puro DG (2005). Regulation of $P2X_7$-induced pore formation and cell death in pericyte-containing retinal microvessels. *Am J Physiol Cell Physiol* **288**, C568–C576.

Sugiyama T, Kobayshi M, Kawamura H, Li Q & Puro DG (2004). Enhancement of $P2X_7$-induced pore formation and apoptosis: an early effect of diabetes on the retinal microvasculature. *Invest Ophthalmol Vis Sci* **45**, 1026–1032.

Takagi C, Bursell SE, Lin YW, Takagi H, Duh E, Jiang Z, Clermont AC & King GL (1996). Regulation of retinal hemodynamics in diabetic rats by increased expression and action of endothelin-1. *Invest Ophthalmol Vis Sci* **37**, 2504–2518.

Tilton RG (1991). Capillary pericytes: perspectives and future trends. *J Electron Microsc Tech* **19**, 327–344.

Tilton RG, LaRose LS, Kilo C & Williamson JR (1986). Absence of degenerative changes in retinal and uveal capillary pericytes in diabetic rats. *Invest Ophthalmol Vis Sci* **27**, 716–721.

Walker EH, Pacold ME, Perisic O, Stephens L, Hawkins PT, Wymann MP & Williams RL (2000). Structural determinants of phosphoinositide 3-kinase inhibition by wortmannin, LY294002, quercetin, myricetin, and staurosporine. *Mol Cell* **6**, 909–919.

Wu DM, Kawamura H, Sakagami K, Kobayashi M & Puro DG (2003). Cholinergic regulation of pericyte-containing retinal microvessels. *Am J Physiol Heart Circ Physiol* **284**, H2083–H2090.

Wu DM, Miniami M, Kawamura H & Puro DG (2006). Electrotonic transmission within pericyte-containing retinal microvessels. *Microcirculation* (in press).

Xie LH, John SA, Ribalet B & Weiss JN (2005). Long polyamines act as cofactors in PIP2 activation of inward rectifier potassium (Kir2.1) channels. *J Gen Physiol* **126**, 541–549.

Yamanishi S, Katsumura K, Kobayashi T & Puro DG (2006). Extracellular lactate as a dynamic vasoactive signal in the rat retinal microvasculature. *Am J Physiol Heart Circ Physiol* **290**, H925–H934.

Ye XD, Laties AM & Stone RA (1990). Peptidergic innervation of the retinal vasculature and optic nerve head. *Invest Ophthalmol Vis Sci* **31**, 1731–1737.

Zaritsky JJ, Eckman DM, Wellman GC, Nelson MT & Schwarz TL (2000). Targeted disruption of Kir2.1 and Kir2.2 genes reveals the essential role of the inwardly rectifying K^+ current in K^+-mediated vasodilation. *Circ Res* **87**, 160–166.

Zhang H, He C, Yan X, Mirshahi T & Logothetis DE (1999). Activation of inwardly rectifying K^+ channels by distinct PtdIns(4,5)P_2 interactions. *Nat Cell Biol* **1**, 183–188.

Zhao HB & Santos-Sacchi J (1998). Effect of membrane tension on gap junctional conductance of supporting cells in Corti's organ. *J Gen Physiol* **112**, 447–455.

Acknowledgements

The authors thank Bret Hughes, Anatoli Lopatin, Shigeki Yamanishi and David Wu for helpful discussions. This work was supported by grants from the NIH (EY12505 and EY07003), the Japan Eye Bank Association, the Osaka Medical Research Foundation For Incurable Diseases, and Japan Foundation for Aging and Health. D.G.P. is a Research to Prevent Blindness Senior Scientific Scholar.